ChemComm

Enhanced Seebeck Coefficient of Thermocells by Heat-Induced Deposition of I3−/Hydrophobized α-Cyclodextrin Complexes on Electrode

Journal:	*ChemComm*
Manuscript ID	CC-COM-04-2020-002356.R2
Article Type:	Communication

COMMUNICATION

Enhanced Seebeck Coefficient of Thermocells by Heat-Induced Deposition of I_3^-/Hydrophobized α-Cyclodextrin Complexes on Electrode

Received 00th January 20xx,
Accepted 00th January 20xx

DOI: 10.1039/x0xx00000x

Hirotaka Inoue,[a] Yimin Liang,[a] Teppei Yamada,*[a,b] Nobuo Kimizuka[1,2]

Ethylated α-cyclodextrin (Et_{18}-α-CD) is used as a host matrix for the I^-/I_3^- thermocells. Although Et_{18}-α-CD is not soluble in water at ambient temperature, it becomes soluble by complexation of the I_3^- anion. Meanwhile, the complex is precipitated upon elevating the temperature. The thermo-responsive solubility change of the I_3^-/Et_{18}-α-CD complex increases the Seebeck coefficient (S_e) of the thermocell up to 2.6 mV/K. The underlying mechanism of the increased S_e is elucidated by UV-vis, Raman spectroscopy, and electrochemical measurements. This result shows the temperature-dependent solubility changes of redox-active species as a potential means to improve the performance of electrochemical thermocells.

Thermoelectric conversion attracts much interest recently due to the impending depletion of fossil resources and the pressing demand for their efficient usage. Thermocell has been emerging as an alternative thermoelectric device.[1–3] It consists of a pair of redox species in electrolyte solutions that create an electrochemical potential as a result of the shift of redox equilibrium potentials caused by the temperature difference between two electrodes. The thermoelectric conversion efficiency of a themocell is compared by the figure of merit (*ZT*) expressed as Eq. 1 below;

$$ZT = \frac{\sigma S_e^2}{\kappa} T \quad \text{(Eq. 1)}$$

where σ is electrical conductivity, S_e is Seebeck coefficient, κ is thermal conductivity, and T is the temperature of a cell. Since *ZT* is proportional to the square of S_e, the improvement of S_e plays an important role in enhancing the performance of a thermocell. The thermoelectric conversion efficiency has been improved as reported for hexacyanoferrate redox couples, which showed a Seebeck coefficient (S_e) of −1.43 mV/K and marked 3.95% of the Carnot efficiency.[4] The *ZT* value of 1 is regarded as a milestone for thermoelectric conversion devices, and it would be achieved by increasing the S_e value up to 3.5 mV/K.

S_e of thermocell is proportional to the entropy change between redox reaction, and to date, various strategies have been devoted to improving the S_e of thermocells, such as spin-state transition,[5–8] solvent effect,[9–13] and vaporizing entropy.[14,15] We have introduced host-guest interactions to the I^-/I_3^- thermocells, and reported the S_e of ca. 2.0 mV/K by introducing α-CD.[16–18] S_e of a thermocell is defined as the shift of redox equilibrium potential divided by the temperature difference, and accordingly, much larger S_e can be achieved by the drastic change in a small temperature range. To provide such thermo-response to electrodes, we focus on the control of the electrochemical reaction mechanism of guest redox species by taking advantage of the solubility switching of the host-guest complexes. It is performed by the modification of a redox species by heat-induced deposition of I_3^-/host complexes onto an electrode. The deposited complexes unexpectedly exerted through-bond electron transfer, which caused shifts in the equilibrium potential as compared to the corresponding

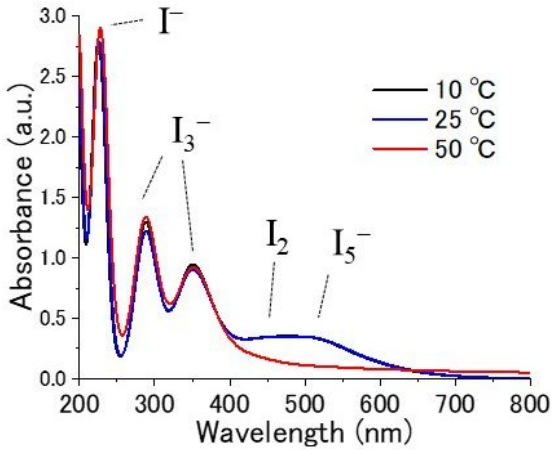

Figure 1. UV-vis spectra of Et_{18}-α-CD and polyiodide at varied temperatures.

[a] *Division of Chemistry and Biochemistry, Graduate School of Engineering, Kyushu University, Motooka 744, Nishi-ku, Fukuoka 819-0395, Japan.*
[b] *Center for Molecular Systems, Kyushu University.*
Electronic Supplementary Information (ESI) available: [Details of experiments and supplemental figures]. See DOI: 10.1039/x0xx00000x

electrochemical reaction in bulk solution. To carry out such temperature-responsive electrode modification, we found that an Et_{18}-α-CD (Hexakis(2,3,6-tri-*O*-ethyl)-α-cyclodextrin) fulfills the requirement for the host compound. Et_{18}-α-CD is a hydrophobic compound and is not soluble in water, whereas it becomes water-soluble upon the uptake of I_3^- anion in the cavity. With increasing temperature, Et_{18}-α-CD-I_3^- composite showed precipitation by overwhelming hydrophobic interactions. The present thermo-responsive Et_{18}-α-CD-based I^-/I_3^- thermocell showed a significant increase in S_e up to 2.6 mV/K. To our knowledge, this is the first report on the thermo-responsive deposition of electroactive host-guest complexes that served to enhanced hydrophilicity of the complex by the inclusion of I_3^- ion. Interestingly, precipitation of the complex was observed with increasing temperature. As shown in Fig. S1, a gradual decrease of transmittance was observed above 20 °C, which is followed by a steep drop around at ca. 40 °C. A drastic change of color was also visually observed at 46 °C due to the precipitation (Fig. S2, Fig. S3-b). The heat-induced formation of larger aggregates in solution was also confirmed by DLS measurement (Fig. S4). As is well known, alkyl groups are hydrophobically hydrated in aqueous solution, which shows entropy-driven dehydration upon increasing temperature. This would be responsible for the observed heat-induced precipitation of Et_{18}-α-CD above 40 °C.

To analyze the iodine species dissolved in the aqueous mixture, UV-vis spectra were measured at various temperatures (Fig. 1 and S5). At 10 °C, absorption peaks were observed at 225, 288 and 352 nm together with a broad absorption from 450 to 700 nm. The peak at 225 nm is assignable to the I^- ion,[20,21] and the peaks at 288 and 352 nm are assigned to I_3^- species dissolved in water.[22–25] Meanwhile, the maximum of the broad peak at 505 nm is assigned to I_5^- anion.[18] We have previously reported that I_5^- anion is formed explicitly in solution by inclusion in methylated α-CDs,[18] and we accordingly consider that Et_{18}-α-CD acquired the solubility in water by uptaking I_5^- ion at low temperatures. Upon increasing temperature to 50 °C, the peak intensity at 505 nm was decreased, reflecting the heat-induced precipitation phenomena. As the absorption peak at 288 nm shows an increase at higher temperatures, it is possible that the I_5^- ions in Et_{18}-α-CD is released to bulk water as I_3^- ions, according to Eq. 1.

$$Et_{18}\text{-α-CD-}I_5^- + I^- \rightarrow 2I_3^- \quad \text{(Eq. 1)}$$

We have confirmed that the I_3^- ion is contained in the precipitated Et_{18}-α-CD, as supported by the Raman spectral measurement described later.

Thermo-electric measurement was then performed using H-shape glassware.[16] Figure 2 shows a thermoelectric potential curve without (a) or with 0.5 mM Et_{18}-α-CD (b). The thermocell without the host showed a S_e of 0.73 mV/K, which is consistent with the previous study (a). On the other hand, that with Et_{18}-α-CD showed complex temperature dependence (b). At low temperature, the S_e observed in the presence of Et_{18}-α-CD is ca. 0.8 mV/K (b), which is comparable to that of I^-/I_3^- without the host (a).[16] In the previous reports, the addition of a small amount of the host compared to I_3^- anion exerted a negligible

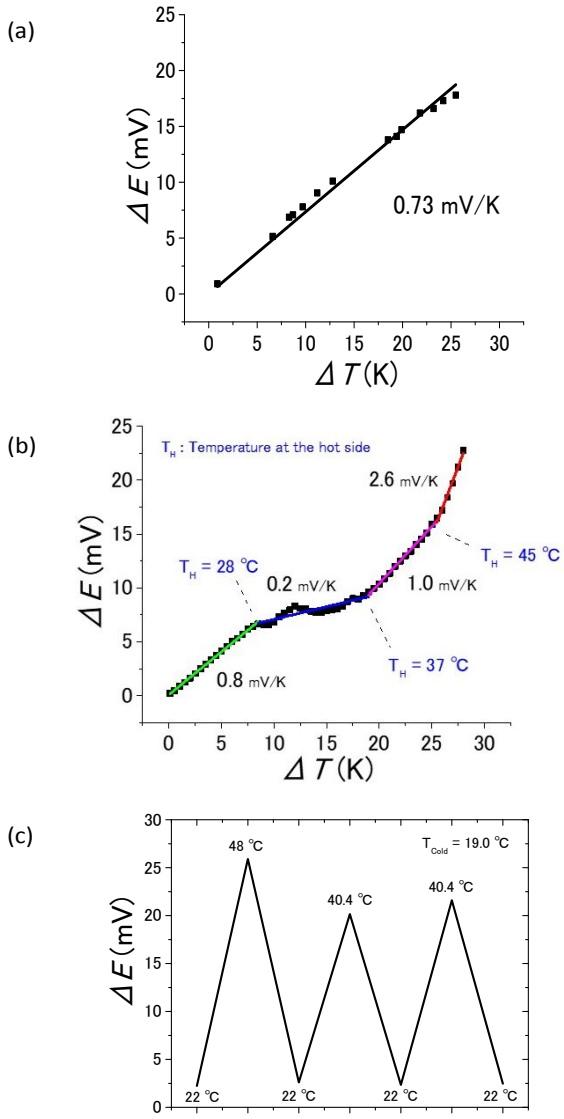

Figure 2. Thermoelectric voltage measurement along with the temperature difference (a) without host and (b) with Et_{18}-α-CD (0.5 mM). [KI] = 10 mM, [KI_3] = 2.5 mM. Temperature of the cold side was kept at 19.5 °C. (c) Cycle test of thermoelectric voltage measurement.

effect on S_e.[17] Upon increasing the temperature difference between both electrode cells from 8 to 18 K, the S_e value turned to a smaller average value of 0.2 mV/K. Meanwhile, the slope increases again by further heating above 20 K, and finally reached a high S_e value of ca. 2.6 mV/K. As mentioned previously, change in color was observed at 46 °C due to the formation of the precipitate (Fig. S2), which is, however, thermally reversible and the thermoelectric voltages are reproducibly observed during at least three heating and cooling cycles (Fig. 2c).

These results indicate that the increase in S_e value is associated with the formation of precipitates. We observed the deposition of the precipitates at the surface of the hot-side electrode, which seems to have affected the electrochemical reactions on the hot electrode. To get more insight into the redox reactions occurring at higher temperatures, cyclic voltammetry was conducted by changing temperatures (Fig. 3). The cyclic

voltammogram without the host is shown in Fig. S6 for comparison. An apparent decrease in the peak separation was observed between the reduction and oxidation peaks by elevating the temperature, where the shift of $E^{1/2}$ is ca. 1.0 mV/K. As $E^{1/2}$ can be regarded as an equilibrium potential, S_e is estimated as ca. 0.8 mV/K by considering the temperature effect on the potential of Ag/AgCl electrode (ca. 0.2 mV/K)[26]. This S_e value is in good agreement with that obtained by the thermoelectric measurement.

In the presence of Et_{18}-α-CD, the oxidation peak was observed at ca. 0.60 V vs. Ag/AgCl, and the peak potential showed a moderate shift upon increasing the temperature. On the other hand, a significant shift was observed for the reduction peak. At low temperature, the peak exists at 0.28 V, which is assigned to the reduction of I_3^-. With the increase of temperature above 35 °C, the peak shifts to the positive direction with decreasing intensity and reached a peak at 0.38 V (temperature, 45 °C). This shift of the reduction potential is associated with the precipitation. The hot electrode is covered with the precipitates, in which the presence of I_3^- was confirmed by Raman spectroscopy (Fig. S7). Despite the precipitation, the diffusion of the reductant is not the rate-determining step at the hot side, as indicated by the shift in the reduction potential. This is in remarkable contrast to the cold-electrode side of the thermocell, in which the redox reaction occurred in homogeneous solution and the I_3^- anion encapsulated by Et_{18}-α-CD is not engaged in the electrochemical reaction.

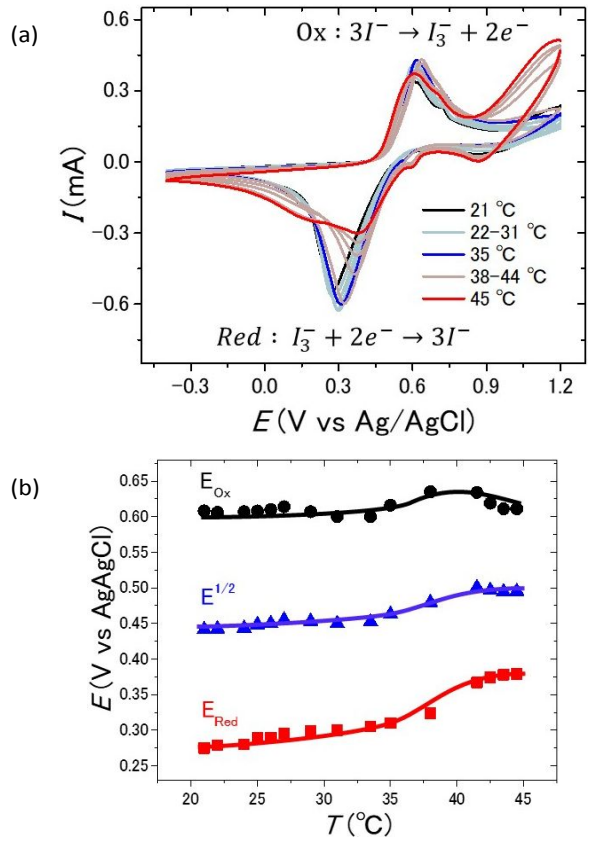

Figure 3. (a) Cyclic voltammograms of I^- (10 mM) and I_3^- (2.5 mM) in the presence of Et_{18}-α-CD (0.5 mM). 100 mM of KNO_3 was added for supporting electrolyte. (b) The plot of $E_{1/2}$ and peak potential of reduction reactions at various temperatures.

In addition, the energy level of I_3^- incorporated in Et_{18}-α-CD is slightly different from that without the host, as observed by UV spectra (Fig. S8). The I_3^- peak is observed at ca. 288 nm with no host, which shifted to ca. 289.5 nm in the presence Et_{18}-α-CD, indicating the decrease of the HOMO-LUMO gap of ca. 22 meV upon complexation. The shift would also be related to the change in the redox peak. Meanwhile, I^- anions dissolved in the solution at both sides of the hot and cold-electrode cell almost equally contribute to the oxidation reactions and consequently showed only moderate a shift by the temperature change. As a result, the $E^{1/2}$ is mainly affected by the large shift of the reduction reaction which was induced by the precipitation. It is to note that the change of $E^{1/2}$ was observed at ca. 34 °C, which has also been noticed in the transmittance change shown in Fig. S1. The precipitate formation is promoted by the addition of KNO_3 in CV measurement that increased the dielectric constant of the solvent. Without KNO_3, the precipitation was observed at 46 °C, while it was observed between 34 and 39 °C with KNO_3 (Fig. S3). This result is in good agreement with the CV and thermocell measurements.

The current and power output of the thermocell with and without the host was evaluated by current-voltage measurement (Fig. 4 and S9). The maximum power output increases when a larger temperature difference existed between the two electrodes. Since the power (P) is proportional to the square of temperature difference, $P/\Delta T^2$, which was proportional to the square of the Seebeck coefficient,[9] was also plotted in Fig. 4b. Although the maximum power is deviated by measurement temperature, the peak $P/\Delta T^2$ value decreases by increasing the temperature from 24.2 to 33.4 °C and increases with further heating. This trend is the same as that of the Seebeck coefficient. This result supports the change of the Seebeck coefficient by various temperatures. The resistance of the cell was evaluated from I-V to be 3-4 kΩ, which is almost the same as that without the host (Fig. S9). This indicates that the host-guest reaction and formation of the precipitate do not affect to current output.

In this research, a heat-induced deposition reaction along with the hydrophobic hydration was combined with a redox reaction and achieved the arguably-high Seebeck coefficient. Two strategies can be applicable for achieving the combination. One is to introduce functional groups causing hydrophobic hydration into a redox-active molecule. However, this strategy may require a complicated design of the molecule. The other is to use a host molecule for the redox species that shows hydrophobic hydration. The latter case has degrees of freedom of the combinations of redox pair and its host, including one that reported in the manuscript.

Conclusions

Et_{18}-α-CD was newly synthesized and temperature-responsive phenomena were investigated. Et_{18}-α-CD captures triiodide and dissolved in water, and it precipitates with increasing temperature. In the presence of Et_{18}-α-CD, S_e changes step by step with changing the temperature. Whereas at low temperature, S_e is almost the same the result in the case of no

(a)

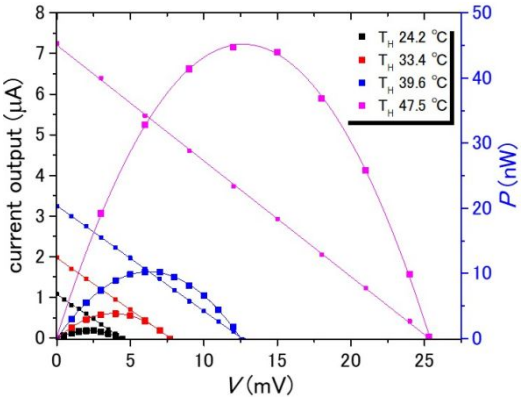

(b)

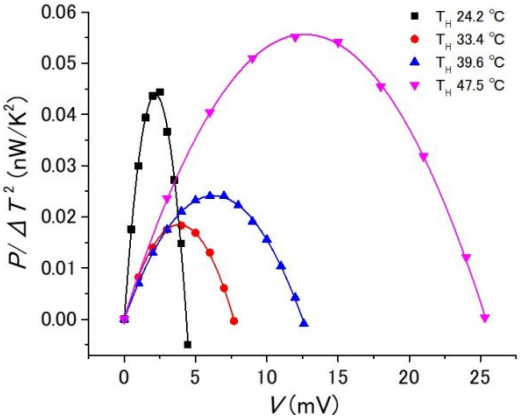

Figure 4. (a) I–V and P–V plots of a thermocell at various temperatures at the hot electrode side. The temperature at the cold side was fixed at ca. 19.5 °C. (b) P/ΔT²–V plots of a thermocell

host (ca. 0.8 mV/K), at elevated temperature, it turns small (ca. 0.2 mV/K) and finally largely increases up to ca. 2.6 mV/K. The mechanism of the result was investigated by spectroscopic and electrochemical measurements with varying temperature. These measurements show that the reduction potential is affected by the deposition of Et_{18}-α-CD-I_3^- complex onto the hot electrode, which causes the improvement of S_e. This result reveals the utility of temperature-responsive electrode deposition for thermoelectric conversion. To our knowledge, this is the first report on the temperature-responsive surface modification of the electrode. Various temperature-responsive polymers or phenomena were reported, and by the combination with the electrode modification, this method could be a powerful method for thermocells.

Conflicts of interest

There are no conflicts to declare.

Acknowledgement

This work was partly supported by JST PRESTO Grant Number JPMJPR141D, JSPS KAKENHI Grant Numbers JP25220805, JP17H03046, JP19H05061(Hydrogenomics), JP16H06513 (Coordination Asymmetry). The authors would like to show our appreciations to the financial support from Ogasawara Foundation for the Promotion of Science & Engineering, "Innovation inspired by Nature" Research Support Program, SEKISUI CHEMICAL CO. LTD and The Thermal & Electric Energy Technology Foundation.

Notes and references

1 T. I. Quickenden and Y. Mua, *J. Electrochem. Soc.*, 1995, **142**, 3985.
2 A. Gunawan, C. H. Lin, D. A. Buttry, V. Mujica, R. A. Taylor, R. S. Prasher and P. E. Phelan, *Nanoscale Microscale Thermophys. Eng.*, 2013, **17**, 304–323.
3 M. F. Dupont, D. R. MacFarlane and J. M. Pringle, *Chem. Commun.*, 2017, **53**, 6288–6302.
4 H. Im, T. Kim, H. Song, J. Choi, J. S. Park, R. Ovalle-Robles, H. D. Yang, K. D. Kihm, R. H. Baughman, H. H. Lee, T. J. Kang and Y. H. Kim, *Nat. Commun.*, 2016, **7**, 10600.
5 T. J. Abraham, D. R. Macfarlane and J. M. Pringle, *Energy Environ. Sci.*, 2013, **6**, 2639–2645.
6 M. A. Lazar, D. Al-Masri, D. R. MacFarlane and J. M. Pringle, *Phys. Chem. Chem. Phys.*, 2016, **18**, 1404–1410.
7 D. Al-Masri, M. Dupont, R. Yunis, D. R. MacFarlane and J. M. Pringle, *Electrochim. Acta*, 2018, **269**, 714–723.
8 A. Taheri, D. R. MacFarlane, C. Pozo-Gonzalo and J. M. Pringle, *Aust. J. Chem.*, 2019, **72**, 709–716.
9 T. Kim, J. S. Lee, G. Lee, H. Yoon, J. Yoon, T. J. Kang and Y. H. Kim, *Nano Energy*, 2017, **31**, 160–167.
10 J. Duan, G. Feng, B. Yu, J. Li, M. Chen, P. Yang, J. Feng, K. Liu and J. Zhou, *Nat. Commun.*, 2018, **9**, 5146.
11 J. H. Kim, J. H. Lee, R. R. Palem, M.-S. Suh, H. H. Lee and T. J. Kang, *Sci. Rep.*, 2019, **9**, 8706.
12 K. Kim, S. Hwang and H. Lee, *Electrochim. Acta*, 2020, **335**, 135651.
13 D. Inoue, Y. Fukuzumi and Y. Moritomo, *Jpn. J. Appl. Phys.*, 2020, **59**, 037001.
14 H. Zhou and P. Liu, *ACS Appl. Energy Mater.*, 2018, **1**, 1424–1428.
15 H. Ma, X. Wang, Y. Peng, H. Peng, M. Hu, L. Xiao, G. Wang, J. Lu and L. Zhuang, *ACS Energy Lett.*, 2019, 1810–1815.
16 H. Zhou, T. Yamada and N. Kimizuka, *J. Am. Chem. Soc.*, 2016, **138**, 10502–10507.
17 Y. Liang, H. Zhou, T. Yamada and N. Kimizuka, *Bull. Chem. Soc. Jpn.*, 2019, bcsj.20190062.
18 Y. Liang, T. Yamada, H. Zhou and N. Kimizuka, *Chem. Sci.*, 2019, **10**, 773–780.
19 Y. Akae, Y. Koyama, H. Sogawa, Y. Hayashi, S. Kawauchi, S. Kuwata and T. Takata, *Chem. - A Eur. J.*, 2016, **22**, 5335–5341.
20 A. D. Awtrey and R. E. Connick, *J. Am. Chem. Soc.*, 1951, **73**, 1842–1843.
21 S. V. Kireev and S. L. Shnyrev, *Laser Phys.*, , DOI:10.1088/1054-660X/25/7/075602.
22 D. A. Palmer, R. W. Ramette and R. E. Mesmer, *J. Solution Chem.*, 1984, **13**, 673–683.
23 R. C. Troy, M. D. Kelley, J. C. Nagy and D. W. Margerum, *Inorg. Chem.*, 1991, **30**, 4838–4845.
24 Y. Bichsel and U. Von Gunten, *Anal. Chem.*, 1999, **71**, 34–38.
25 V. T. Calabrese and A. Khan, *J. Phys. Chem. A*, 2000, **104**, 1287–1292.
26 A. J. deBethune, T. S. Licht and N. Swendeman, *J. Electrochem. Soc.*, 1959, **106**, 626–627.